ARTICLE
Journal of Cellular Biochemistry 116:1982–1992 (2015)

Journal of Cellular Biochemistry

Gcn5 Modulates the Cellular Response to Oxidative Stress and Histone Deacetylase Inhibition.

Ann-Christin Gaupel,[1,2] Thomas J. Begley,[2,3] and Martin Tenniswood[1,2]*

[1]*Department of Biomedical Sciences, School of Public Health, University at Albany, New York*

[2]*Cancer Research Center, University at Albany, New York*

[3]*Nanobioscience Constellation, SUNY Polytechnic Institute, Colleges of Nanoscale Science and Engineering, Albany, New York*

ABSTRACT

To identify chemical genetic interactions underlying the mechanism of action of histone deacetylase inhibitors (HDACi) a yeast deletion library was screened for hypersensitive deletion mutants that confer increased sensitivity to the HDACi, CG-1521. The screen demonstrated that loss of *GCN5* or deletion of components of the Gcn5 histone acetyltransferase (HAT) complex, SAGA, sensitizes yeast to CG-1521-induced cell death. Expression profiling after CG-1521 treatment reveals increased expression of genes involved in metabolism and oxidative stress response, and oxidative stress response mutants are hypersensitive to CG-1521 treatment. Accumulation of reactive oxygen species and increased cell death are enhanced in the *gcn5Δ* deletion mutant, and are abrogated by anti-oxidants, indicating a central role of oxidative stress in CG-1521-induced cell death. In human cell lines, siRNA mediated knockdown of GCN5 or PCAF, or chemical inhibition of GCN5 enzymatic activity, increases the sensitivity to CG-1521 and SAHA. These data suggest that the combination of HDAC and GCN5/PCAF inhibitors can be used for cancer treatment. J. Cell. Biochem. 116: 1982–1992, 2015.

KEY WORDS: HISTONE DEACETYLASE; GCN5; HISTONE ACETYL TRANSFERASE; OXIDATIVE STRESS; YEAST; MAMMALIAN

Histone deacetylase inhibitors (HDACi) are promising therapeutic agents for treatment of cancer. A variety of natural and synthetic HDACi, including Trichostatin A (TSA), suberoylanilide hydroxamic acid (SAHA), and CG-1521 (7-phenyl-2,4,6- heptatrienoic hydroxamic acid) have been reported to induce apoptosis, cell cycle arrest and anti-tumor immunity and to inhibit angiogenesis in various cancer models [Chatterjee et al., 2013; West and Johnstone, 2014]. Both SAHA (vorinostat) and Romidepsin (Istodex), a cyclic tetrapeptide, have been approved by the FDA for the treatment of cutaneous T-cell lymphoma [Mann et al., 2007; VanderMolen et al., 2011]. While monotherapies with HDACi in solid tumors generally lack significant therapeutic efficacy, combination therapies have better clinical outcomes [Qiu et al., 2013; Slingerland et al., 2014], highlighting the need to develop potent combination treatments.

Characterization of the negative chemical-genetic interactions with CG-1521 in *Saccharomyces cerevisiae* has demonstrated that deletion of *GCN5* and other components of the GCN5 histone acetyltransferase (HAT) complex confers hypersensitivity to CG-1521 [Gaupel et al., 2014]. GCN5 is the catalytic subunit of the yeast HAT complexes ADA, SAGA and SLIK [Grant et al., 1997; Eberharter et al., 1999]. The human homologues, GCN5 and its paralogue PCAF (p300/CBP associated factor), are the HAT components of the human ATAC and SAGA complexes. HATs have also emerged as potential targets for the treatment of cancer [Dekker and Haisma 2009] and inhibitors have been developed for p300/CBP, PCAF, and GCN5, including natural products such as curcumin and garcinol as well as synthetic small molecule compounds such as isothiazolones and α-methylene-γ-butyrolactones [Dekker and Haisma 2009].

The current manuscript describes the use of yeast mutant screens to identify novel molecular targets of HDACi, and the validation of these targets in human cancer cell lines, exemplified by HT-29 colorectal cells. The data demonstrate HDACi induce oxidative stress response in both yeast and mammalian cell culture models through a process modulated by GCN5. Coordinated inhibition of HDACs and HATs enhances ROS- mediated cell death in mammalian cancer cells, indicating that combination treatment may provide a new therapy for a number of cancers.

Ann-Christin Gaupel's present address is Deutsches Krebsforschungszentrum, Heidelberg

*Correspondence to: Dr. Martin Tenniswood, Cancer Research Center, University at Albany, 1 Discovery Drive, Rensselaer, NY 12144.

E-mail: mtenniswood@albany.edu

Manuscript Received: 1 March 2015; Manuscript Accepted: 3 March 2015

Accepted manuscript online in Wiley Online Library (wileyonlinelibrary.com): 9 March 2015

DOI 10.1002/jcb.25153 • © 2015 Wiley Periodicals, Inc.

METHODS

YEAST STRAINS AND CELL LINES

The *gcn5* deletion strain from the *S. cerevisiae* library (Open Biosystems, Thermo Scientific, Hudson, NH), established by the Yeast Deletion Consortium, on the BY4741 background (Genotype: *MATa his3Δ1 leu2Δ0 met15Δ0 ura3Δ0*) and the parental strain, transformed with pYE13G (American Type Culture Collection), conferring G418 resistance, was used in YPD growth media containing G418, as previously described [Begley et al., 2004]. HT-29 colorectal adenocarcinoma cells were grown in RPMI-1640 (Gibco, Grand Island, NY) containing 10% fetal bovine serum. Cells were passaged every 3–4 days.

SPOT AGAR ASSAYS

To assess the sensitivity of yeast deletion mutants to hydrogen peroxide, wild-type and *gcn5Δ* yeast strains were spotted on agar plates containing 3 mM H_2O_2 (Sigma-Aldrich, St. Louis, MO). Different cell concentrations were spotted using 1:20 serial dilution and the plates were incubated for 60 h and then imaged. Sensitivity was scored by comparison to the untreated cells, essentially as described previously [Gaupel et al., 2014].

The protective effect of antioxidants was tested in liquid culture using 96-well plates. N-acetylcysteine (NAC, Sigma-Aldrich) was dissolved in phosphate buffered saline (PBS) and the pH was adjusted to pH 7.4. 195 μL YPD containing the indicated concentrations of CG-1521 and N-acetylcysteine were inoculated with 5 μL cell suspension. After 20 h incubation, the cell suspension was diluted 1:2 and the OD_{600} was measured. The ratio treated/untreated was calculated.

ASSESSMENT OF SENSITIVITY OF MAMMALIAN CELLS

HT-29 cells were seeded at 2000 cells/well in 96-well plates and treated after 48 h with the indicated concentrations of CG-1521 (Errant Gene Therapeutics, Chicago, IL) and SAHA (LC Laboratories, Woburn, MA), the specific Gcn5 inhibitor MB-3 (Sigma-Aldrich) or vehicle control (DMSO) in the presence or absence of N-acetylcysteine (Sigma-Aldrich). Cells were fixed in 3.7% formaldehyde for 20 min and washed PBS containing 0.9 mM $CaCl_2$ and 0.5 mM $MgCl_2$. Nuclei were stained with Hoechst 33258 and the nuclei count was determined using the IN Cell Analyzer 2200 and IN Cell Analyzer Workstation 3.7 (GE Healthcare Life Sciences, Pittsburgh, PA). The data were normalized to control and are presented as fraction of control.

SIRNA KNOCKDOWN

HT-29 cells were plated at 2,500 cells/well in 96-well plates and transfected with siGENOME SMARTpool® siRNA for Gcn5 and PCAF or the siGENOME non-targeting pool #2 24 h after plating using DharmaFECT 1 transfection reagent (Thermo Fisher Scientific, Pittsburgh, PA). Optimal knockdown was achieved with a final concentration of 25 nM siRNA and 0.2 μL/well DharmaFECT 1. 48 h following siRNA knockdown, the cells were treated with HDAC inhibitors. Cell number was determined using the IN Cell Analyzer 2200 after treatment with CG-1521, SAHA or vehicle control for 72 h as described above. Cell viability was also determined using alamarBlue® (Molecular Probes, Thermo Fisher Scientific). The data were normalized to the vehicle control (Ratio = treated/control) and subsequently to the non-targeting control (Ratio target siRNA/Ratio non-targeting siRNA). Experiments in 6-well plates to determine knockdown efficiency by immunoblot or quantitative Real-Time PCR were scaled up using 4 μL/well DharmaFECT 1. RNA and protein were harvested 24 h and 72 h after transfection, respectively.

QUANTITATIVE REAL-TIME PCR ANALYSIS

Exponentially growing cultures of BY4741 wild-type strain were treated for 1 h and 2 h with 50μM CG- 1521 or the vehicle control DMSO. RNA was extracted using the mRNeasy mini kit (Qiagen) after enzymatic lysis of the yeast cell wall using zymolyase. 20×10^6 yeast cells were resuspended in Buffer Y1 containing 0.1% β-mercaptoethanol and 25 U zymolyase and incubated at 30°C for 20–30 min.

HT-29 cells were plated at 160,000 cells/well in 6-well plates. RNA from HT-29 cells was harvested 24 h after knockdown. Cells were lysed and RNA was extracted using the Qiagen mRNeasy mini kit. The RNA concentration was measured using the NanoDrop (Thermo Fisher Scientific). Reverse transcription reactions were performed using Taqman Reverse Transcription Reagents (Applied Biosystems, Life Technologies, Carlsbad, CA) to synthesize cDNA. qPCR primers were designed using Primer-Blast (National Center for Biotechnology Information) or Primer3 (Whitehead Institute for Biomedical Research) [Rozen and Skaletsky 2000]. The primer sequences are tabulated in Supplemental Table S1. qRT-PCR reactions were prepared using SYBR Green PCR Master Mix (Applied Biosystems) and analyzed on ABI 7900HT Fast Real-Time PCR System (Applied Biosystems). Relative expression levels normalized to an endogenous reference gene (actin (yeast) and 18S rRNA (HT-29 cells)) were analyzed using $2^{-\Delta\Delta Ct}$ method and log2 transformed [Livak and Schmittgen 2001]. The data represent three independent biological replicates (mean ± SD, $P < 0.05$). Heatmaps were generated using average-linkage hierarchical clustering (Cluster version 2.11) and illustrated using Treeview version 1.60 (http://rana.lbl.gov/EisenSoftware.htm) [Eisen et al., 1998].

IMMUNOBLOT ANALYSIS

Cells were harvested 48–72 h after knockdown by washing with cold PBS containing 0.9 mM $CaCl_2$ and 0.5 mM $MgCl_2$ and lysed in Laemmli buffer supplemented with 5% β-mercaptoethanol. Cell lysates were incubated at 95°C for 5 min and sonicated three times for 10 s. Total cell lysates were separated by SDS-PAGE and transferred to PVDF membranes using wet transfer. Membranes were immunoblotted with antibodies raised against GCN5 (rabbit mAb, Cell Signaling Technology, Danvers, MA, C26A10, 1:1000), PCAF (rabbit mAb, Cell Signaling Technology C14G9, 1:1000) and α-tubulin (rat mAb, AbD Serotec, Bio-Rad, Raleigh, NC, clone YOL1/34 MCA78G, 1:15,000). Specific antibody binding was detected using goat anti-rabbit IgG (Bio-Rad, Hercules, CA, cat# 170-6515, 1:5,000) or goat anti-rat IgG (Santa Cruz Biotechnology, Dallas, TX, sc-2303, 1:10,000) secondary antibodies conjugated with horseradish peroxidase using Amersham ECL Plus Western Blotting Reagent (GE Healthcare Life Sciences) and scanned on the Storm-860 imager (GE Healthcare). The band intensities were analyzed with ImageJ

(National Institutes of Health) software and differences in protein levels were normalized to the loading control (α-tubulin).

FLOW CYTOMETRY

Yeast cells, growing in log phase, were treated with 50 μM CG-1521, 3 mM H_2O_2 or vehicle control and aliquots were taken at the indicated times. The cell suspension was pelleted, washed and resuspended in phosphate buffered saline and incubated with 1.5 μM propidium iodide (PI, Sigma-Aldrich) for 10 min, 4μM hydroethidine (HE, Molecular Probes, Thermo Fisher Scientific) for 15 min at 30°C or 10 μM 2′,7′-dichlorodihydrofluorescein diacetate (H2DCFDA, Molecular Probes, Thermo Fisher Scientific) for 30 min at 30°C in the dark. Cells were immediately transferred on ice and PI, ethidium or DCFDA staining was quantitated by flow cytometry analysis using a BD LSR2 flow cytometer (BD Biosciences, San Jose, CA).

HT-29 colorectal cancer cells were seeded in 6-well plates and treated 48 h after plating or siRNA knockdown with CG-1521, SAHA and MB-3 at the indicated concentrations, or vehicle control, for the indicated times. Cells were washed with PBS containing 0.9 mM $CaCl_2$ and 0.5 mM $MgCl_2$, incubated with 5 μM DCFDA in PBS containing Ca^{2+} and Mg^{2+} for 30 min, trypsinized and resuspended in PBS for analysis. DCFDA intensity was measured using flow cytometry.

For all flow cytometry experiments 10,000–20,000 events were recorded. The data were analyzed using FloJo™ software (TreeStar, Ashland, OR). The percentage of PI-, DCFDA- and HE- positive yeast cells was determined. In HT-29 cells, the shift in fluorescence intensity following DCFDA staining was determined as median fluorescence intensity. The median fluorescence intensity following treatment was normalized to that of the control and is shown as fraction of control.

STATISTICAL ANALYSIS

For all experiments, three or more independent biological replicates were performed. The results are presented as mean ± SD. Results are regarded significant if $P < 0.05$ as established by ANOVA and Tukey–Kramer post-test. The overlap of CG-1521- sensitive and oxidative stress–sensitive strains was established using Venn diagrams. Data on strains that show decreased resistance to either oxidative stress, hydrogen peroxide or paraquat were downloaded from the *Saccharomyces* Genome Database on 2013-5-13 and 2014-2-13, respectively [Cherry et al., 2011]. Hyperoxia-sensitive strains were obtained from Outten et al., 2005. The statistical significance and representation factor was calculated using the following website (http://nemates.org/MA/progs/overlap_stats.html).

RESULTS

CG-1521–INDUCED CELL DEATH IS CAUSED BY THE ACCUMULATION OF REACTIVE OXYGEN SPECIES IN THE S. CEREVISIAE GCN5Δ DELETION MUTANT

Chemical genetic profiling of CG-1521 has previously identified the SAGA complex as an important negative regulator of the growth-inhibitory effect of CG-1521 and deletion of its HAT component Gcn5 sensitizes yeast cells to CG-1521-induced cell death [Gaupel et al., 2014]. Gene expression profiling after CG-1521 treatment in yeast suggests that the HDACi induces oxidative stress, decreases respiration and increases glucose scavenging and flow through the pentose phosphate pathway (Fig. 1, panel A). Gene ontology analysis

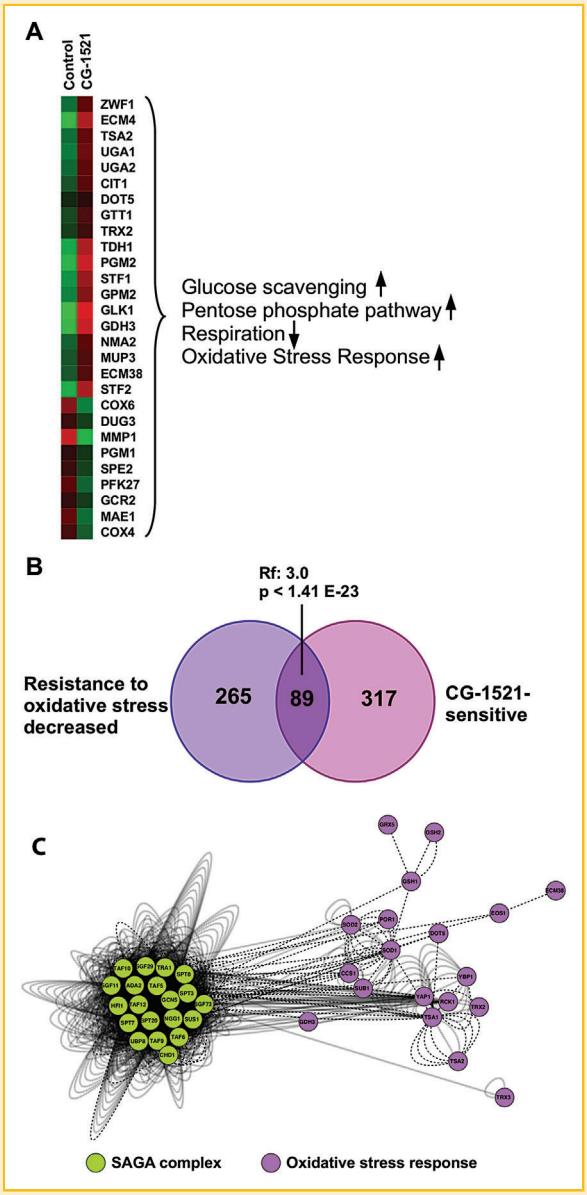

Fig. 1. HDAC inhibition and the oxidative stress response. Panel A: Heatmap of differentially expressed genes after treatment with CG-1521 related to metabolism and oxidative stress was generated using Cluster 2.11 and Treeview 1.60. Panel B: Venn diagram displaying the overlap of CG-1521-sensitive and oxidative stress-sensitive deletion strains. The dataset of deletion mutants with decreased resistance to oxidative stress was downloaded from the Saccharomyces Genome Database on 2013-5-13 [Cherry et al., 2011]. Panel C: Interaction network of the SAGA complex linked to the oxidative stress response generated in cytoscape v 3.0.2 using the BioGRID interaction network release 3.2.109. Edges represent different types of interactions (physical interactions: forward slash: genetic interactions: dash) Green and Purple nodes symbolize components of the SAGA complex or the oxidative stress response, respectively.

identifies an enrichment of GO:0055114 Oxidation/Reduction ($P = 2.1E-5$, Benjamini $P = 9.3E-4$, 18 genes) and GO:0006979 Response to oxidative stress ($P = 8.7E-3$, Benjamini $P = 0.11$, 6 genes). In addition, there is enrichment in GO:0006536, glutamate metabolic processes ($P = 2.5E-3$, Benjamini $P = 4.3E-2$, 4 genes). The expression of glutathione S-transferases with glutaredoxin and glutathione peroxidase activity (Ecm4/Gto2 and Gtt1) [Garcerá et al., 2006] as well as the thioredoxin (Trx2) and peroxiredoxins (Tsa2 and Dot5) increases after CG-1521 treatment. This suggests that CG-1521 represses respiration, potentially limiting the generation of oxidative stress through the electron transport chain. Increased expression of Glk1, Pgm2, and Zwf1 as well as a decrease in Pfk27 expression indicate that glucose is shunted into the pentose phosphate pathway. However, downregulation of purine metabolism (Kegg pathway sce00230, Benjamini $P = 1.4E-2$, 8 genes), as well as upregulation of genes downstream of glyceraldehyde-3-phosphate suggest that the pentose- phosphate pathway is not used for the generation of nucleotides, but rather to increase the NADPH level, which is needed for reductive processes. The differential expression of several of these genes has been confirmed by qRT-PCR analysis (Supplemental Table S2).

Additionally, the yeast deletion mutants with roles in the oxidative stress response (*sod1Δ*, *sod2Δ*, *ccs1Δlys7Δ*, *grx5Δ*, *apd1Δ*, *yap1Δ*, and *sub1Δ*) display sensitivity to CG-1521 (Supplemental Table S3). Comparison of CG-1521-sensitive deletion mutants and deletion mutants that display decreased resistance to oxidative stress indicates an overlap of 89 strains (25% of strains displaying increased sensitivity to oxidative stress are CG-1521-sensitive, $P < 1.41E-23$, representation factor: 3.0) (Fig. 1, panel B). Eighteen percent of deletion mutants that are sensitive to hydrogen peroxide, are also sensitive to CG-1521 (Supplemental Figure 1 Panel A, $P < 8.17E-8$, representation factor: 2.1), while 45% of the deletion mutants, that are sensitive to hyperoxia or the superoxide-inducing agent paraquat, are sensitive to CG-1521 (Supplemental Figure 1 Panel B (paraquat: p,3.54E-17, representation factor: 5.0; hyperoxia: p,7.1E-20, representation factor: 5.4)). This indicates that the effects of CG-1521 are more similar to these two stressors than to hydrogen peroxide.

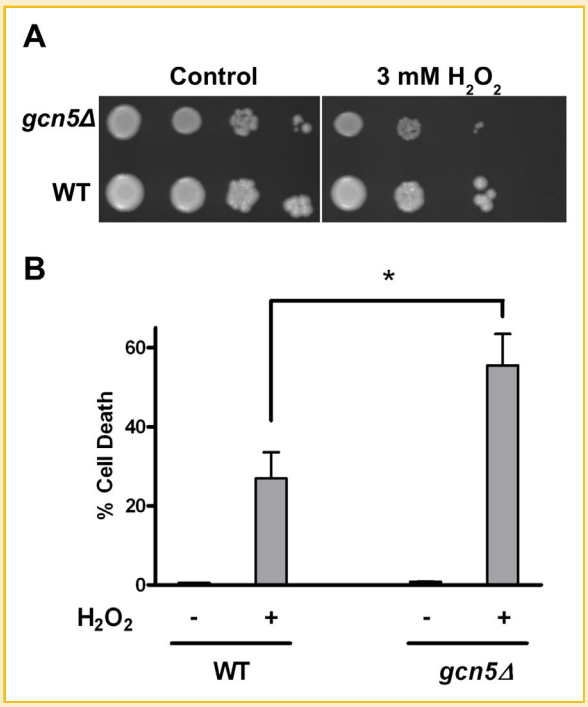

Fig. 2. Deletion of *GCN5* in *S. cerevisiae* increases the susceptibility to hydrogen peroxide-induced cell death. Panel A: Wild-type and *gcn5Δ* strain were spotted on agar plates containing 3 mM hydrogen peroxide. Plates were imaged after 60 h incubation. Representative images of three independent biological replicates are shown. Panel B: Exponentially growing yeast cells were treated with 3 mM hydrogen peroxide for 20 h. Propidium iodide uptake was measured by flow cytometry as described in Methods. The data are presented as mean ± SD of three independent biological replicates and * $P < 0.05$.

While deletion of *GCN5* has not been shown to sensitize *S. cerevisiae* to oxidative stress, studies in *Schizosaccharomyces pombe* and chicken B cells show that Gcn5, and in case of *S. pombe* other SAGA components, are essential for survival to oxidative stress caused by hydrogen peroxide [Kikuchi et al., 2011a]. The cytoscape interaction network, assembled using BioGRID interaction data, confirms a link between the SAGA complex and the oxidative stress response in *S. cerevisiae* and demonstrates that Gcn5 and other SAGA complex components display physical and genetic interactions with several genes involved in the oxidative stress response, including Yap1, Tsa1, Trx3, Sod1, Sod2, Ccs1, Gdh3, and Gsh1 (Fig. 1, Panel C).

To determine if *GCN5* deletion in *S. cerevisiae* sensitizes the cells to hydrogen peroxide, the growth of the wild-type and the *gcn5Δ* strain on agar plates containing 3 mM hydrogen peroxide was assessed. Deletion of *GCN5* only minimally increases the sensitivity of the deletion mutant compared to the wild-type (Fig. 2, Panel A). However, exposure to hydrogen peroxide in liquid culture results in increased cell death as measured by propidium iodide uptake using flow cytometry: 27% of the wild-type cells are propidium iodide positive, compared to 56% of *gcn5Δ* cells, indicating that *GCN5* deletion confers sensitivity to hydrogen peroxide, at least in liquid culture (Fig. 2, Panel B).

Treatment of the wild-type and the *gcn5Δ* deletion mutant with 50 μM CG-1521 leads to an increase in the number of cells showing an accumulation of superoxide after 1 h (7.9%) in the *gcn5Δ* deletion mutant, which further increases to 24% after 3 h. The increase in the percentage of hydroethidine (HE) positive cells in the wild-type strain is delayed and does not reach significance until 3 h (5.5%) (Fig. 3, Panel A). The *gcn5Δ* strain is significantly more sensitive to CG-1521, displaying a greater percentage of DCFDA-positive cells (27%) compared to the wild-type strain (3%) (Fig. 3, Panel B). The growth-inhibitory effects of CG-1521 are abrogated with the antioxidant N-acetylcysteine (NAC) (Fig. 3, Panel C). Treatment with CG-1521 results in a reduction of cell number of the *gcn5Δ* deletion mutant, but not the wild-type after 20 h. Co-treatment with 20 mM or 40 mM NAC rescues the *gcn5Δ* mutant cells from the effects of CG-1521 in a dose-dependent manner (by 2 and 3.7 fold, respectively). At higher concentrations of CG-1521, the wild-type cells are also susceptible to the drug and this effect on the wild-type cells is also rescued by NAC (Fig. 3, Panel C). These results indicate that CG-1521-induced cell death in yeast is mediated in part by

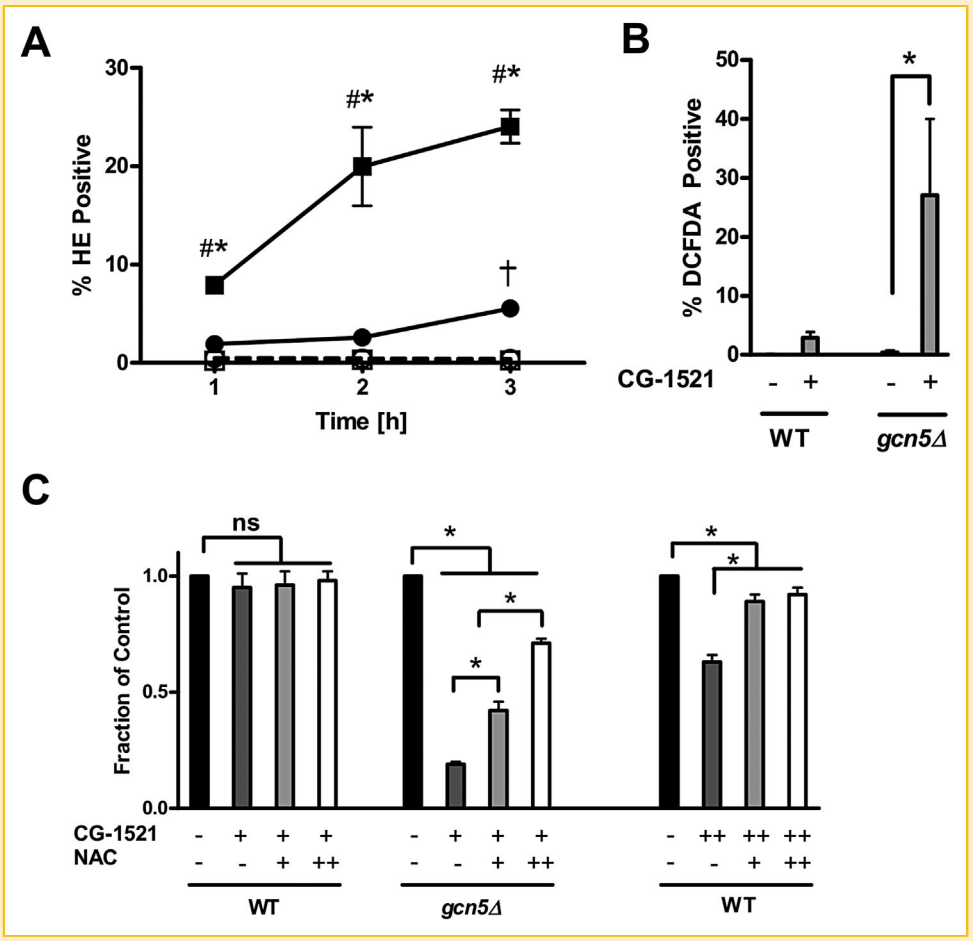

Fig. 3. Enhanced oxidative stress induction after CG-1521 treatment in the gcn5Δ deletion mutant. Panels A: Exponentially growing wild-type and *gcn5Δ* cells were treated with 50 μM CG- 1521, stained with hydroethidine after 1 h to 3 h as described in Methods, The data are shown as mean ± SD, n = 3; $^{\dagger\#*}P < 0.05$. † denotes significance compared to the wild-type control, $^{\#}$ denotes significance compared to the *gcn5Δ* control and * denotes significance of the CG-1521 treated wild-type compared to the CG-1521- treated *gcn5Δ* strain. Panel B: Exponentially growing wild-type and *gcn5Δ* cells were treated with 50 μM CG-1521, stained with DCFDA after 20 h and analyzed with flow cytometry, as described in Methods. The data are shown as mean ± SD n = 3; * $P < 0.05$. denotes significance between CG-1521 treated and control strains. Panel C: YPD containing 25 μM (+) or 50 μM CG-1521 (++) and 20 mM (+) or 40 mM (++) NAC were inoculated with 5 μL cell suspension. After 20 h incubation, the cell suspension was diluted and the OD_{600} was measured. The data were normalized to the control and presented as fraction of control. The data are shown as mean ± SD of three independent biological replicates and $P < 0.05$.

oxidative stress through interaction with the Gcn5 catalytic subunit of yeast HATs.

INHIBITION OR LOSS OF GCN5/PCAF INCREASES THE SENSITIVITY OF COLORECTAL CANCER CELLS TO CG-1521

To determine whether CG-1521 or SAHA can be used in combination with the GCN5 -specific inhibitor, MB-3, as a novel therapeutic option, the effects of CG-1521 or SAHA in combination with MB-3 were tested in HT-29 colorectal cancer cells. These cells have previously been shown to induce apoptosis through induction of oxidative stress in response to SAHA [Portanova et al., 2008]. The EC_{50} at 48 h for CG-1521 and SAHA is approximately 10 μM and 1.75 μM, respectively (Fig. 4, Panels A and B). Combination treatment of CG-1521 (6 μM) or SAHA (1 μM) and MB-3 (50 μM) results in a significant decrease in cell number over the course of 24 h to 72 h, compared to either GCN5 inhibition or HDAC inhibition alone (Fig. 4, Panels C and D). After 72 h of treatment both HDACi decrease the viable cell number compared to untreated controls (CG-1521 to 74% and SAHA to 59%). Treatment with the GCN5-specific inhibitor MB-3 also decreases the proportion of viable cells to approximately 80% of control values after 72 h. Combination treatment with either CG-1521 or SAHA, and MB-3 further decreased the viable cell number to approximately 45% of the untreated controls, indicating that the combination of MB-3 with either HDACi has an additive effect. Similar results were obtained in MCF-7 breast cancer cells (Supplemental Figure S2). These results indicate that GCN5 inhibition sensitizes cancer cells to HDACi. To determine if loss of GCN5 or the homologue PCAF increases the susceptibility to CG-1521 treatment, expression of GCN5 and PCAF was reduced by siRNA knockdown, which results in a decrease of GCN5 and PCAF mRNA expression levels at 24 h (Supplemental Figure S3) and reduces protein expression of GCN5

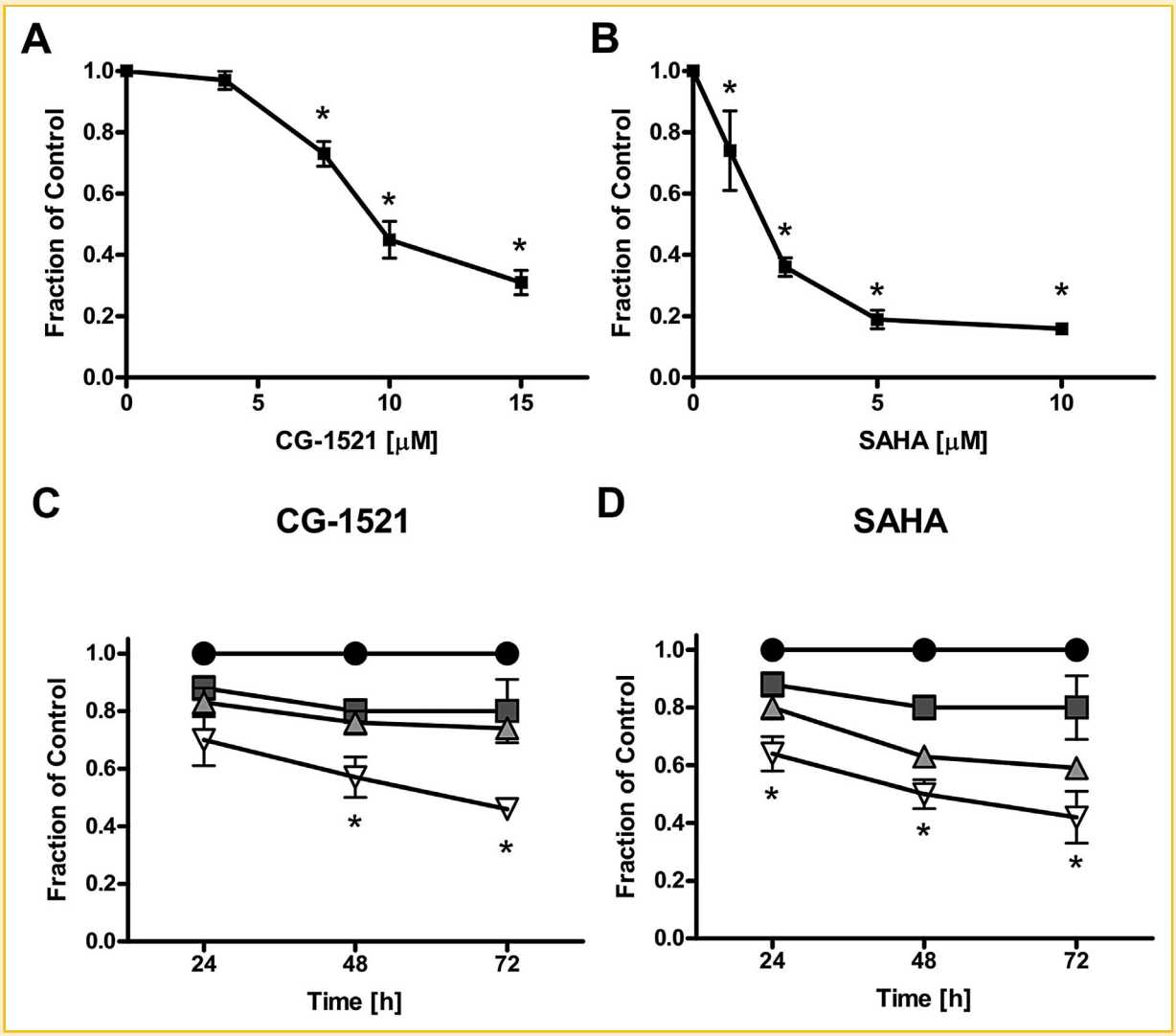

Fig. 4. GCN5 inhibition enhances the growth-inhibitory effect of CG-1521. Panels A and B: HT-29 cells were treated for 48 h with the indicated concentrations of CG-1521 (Panel A) or SAHA (Panel B), fixed, stained with Hoechst and the nuclei count was determined using the GE IN Cell Analyzer 2200. The data were normalized to the untreated control and are presented as fraction of control (mean ± SD of 3 independent biological replicates and * $P < 0.05$) as described in Methods. Panel C and D: HT-29 cells were treated with 6 μM CG- 1521 (Panel C) or 1 μM SAHA (Panel D), 50 μM MB-3 or a combination of HDACi and MB-3 for 24 h to 72 h, fixed, and nuclei were counted on the IN Cell Analyzer 2200. The data were normalized to the control (and presented as fraction of control (mean ± SD and * $P < 0.05$ compared to either agent alone) ($n = 4$ independent biological replicates). Note the experiments were performed at the same time and the control and MB-3 treatment data are replicated in the left and right panels. Control: closed circles; MB-3 alone closed squares; HDACi (CG-1521, panel C; or SAHA, panel D) filled triangles; combination of HDACi and MB-3 open inverted triangles.

and PCAF to approximately 50 and 20% after 72 h, respectively (Fig. 5, Panel A). Similarly, combined knockdown of GCN5 and PCAF decreases their protein expression to 50 and 20%, respectively (Fig. 5, Panel A). Notably, GCN5 knockdown leads to elevated expression of PCAF, as previously shown for chicken DT40 cells [Kikuchi et al., 2005]. Decreased GCN5 and/or PCAF expression is accompanied by reduced growth by approximately 50% compared to the non-targeting control, as measured by nuclei count after 120 h (Supplemental Figure S4). Treatment of HT-29 cells, in which GCN5 and/or PCAF have been knocked down, with CG-1521 for 72 h further decreases the number of adherent cells by 25 to 30% compared to the non-targeting siRNA (Fig. 5, Panel B). SAHA also significantly reduces growth in GCN5, PCAF and GCN5+PCAF siRNA transfected HT-29 cells (Fig. 5, Panel B). Measurement of cell viability using alamarBlue® confirms these results (Supplemental Figure S5), indicating that loss or inactivation of GCN5 and/or PCAF increases the susceptibility to HDACi, exemplified by CG-1521 and SAHA

GCN5 INHIBITION LEADS TO AN ACCUMULATION OF ROS IN HT-29 CELLS

The growth inhibition after CG-1521 treatment is accompanied by increased oxidative stress as shown by DCFDA staining. HT-29 cells were treated with 15 μM CG-1521 and 2.5 μM or 5 μM SAHA, and

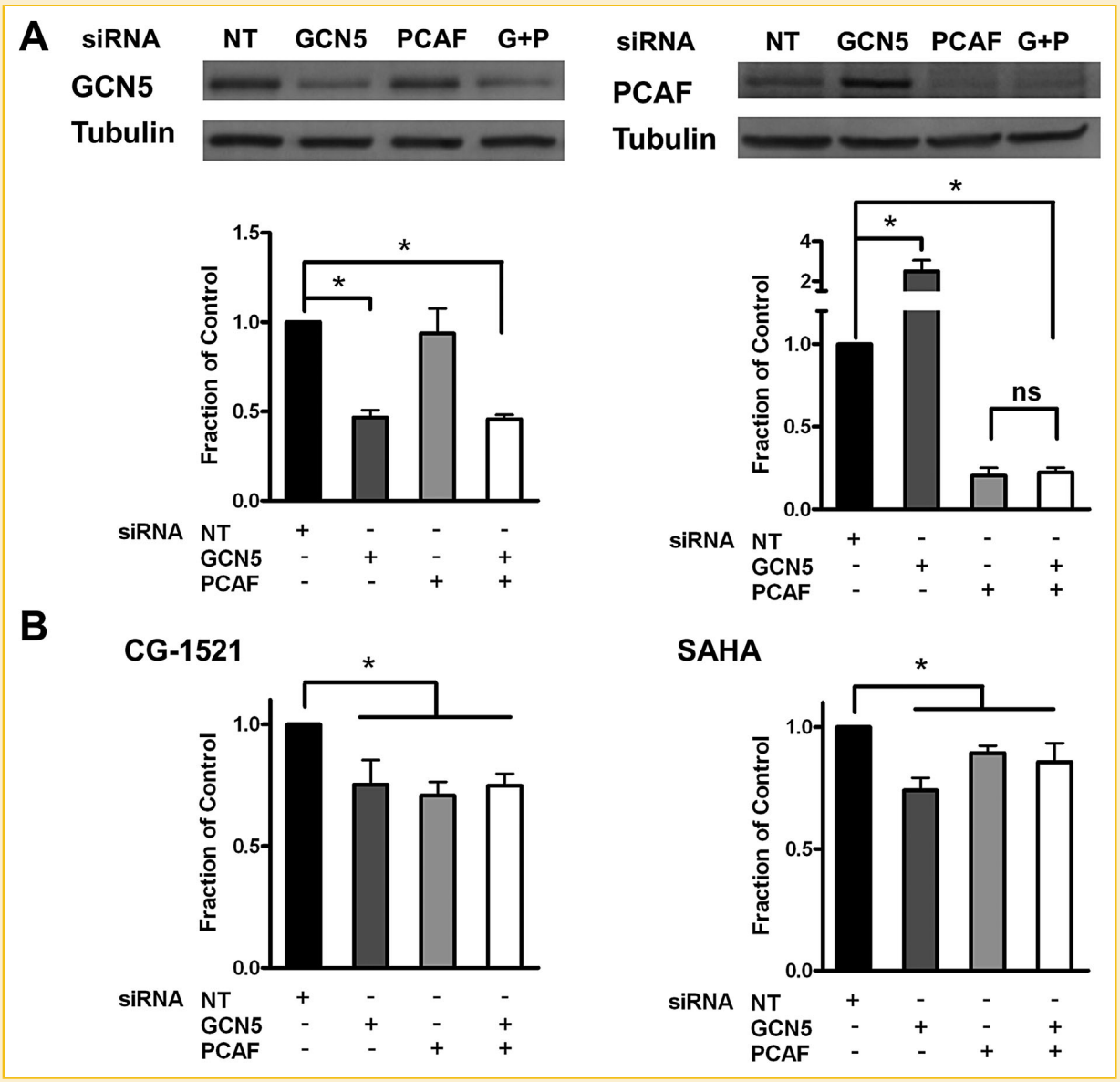

Fig. 5. GCN5 and PCAF knockdown sensitizes HT-29 cells to CG-1521. Panel A: HT-29 total protein was harvested 72 h after siRNA transfection and subjected to immunoblot analysis. GCN5 or PCAF expression was normalized to tubulin and calculated relative to the non-targeting control as described in Methods. Panel B: HT-29 cells were treated 48 h after transfection with 10 μM CG-1521 or 1.75 μM SAHA for 72 h. Cells were fixed and the cell number was determined using the IN Cell Analyzer 2200. To determine significant changes, the cell number was normalized first to the vehicle control and then to the non-targeting (NT) control. The results are presented as mean ± SD of 3-4 independent biological replicates and * $P < 0.05$.

production of ROS was measured by flow cytometry. Compared to the control, oxidative stress levels are increased following CG-1521 treatment by 4.6 fold. A comparable concentration of SAHA (2.5 μM) does not significantly increase oxidative stress, however 5 μM SAHA does, albeit not to the same extent as CG-1521 (Fig. 6). To determine whether the growth-inhibitory effect of CG-1521 is accompanied by increased ROS generation in HT-29 cells with decreased activity or expression of GCN5 or PCAF, as documented in yeast (Fig. 3), levels of oxidative stress were measured after HDAC inhibition and siRNA knockdown of GCN5 or PCAF or MB-3 treatment. GCN5 knockdown and/or combined knockdown of GCN5 and PCAF significantly increases ROS accumulation in HT-29 cells (Fig. 7, Panel A). Only SAHA induces oxidative stress at low concentrations (Fig. 7, Panel A), and the combination of either HDACi with knockdown of either GCN5, PCAF or the combination of GCN5 and PCAF does not result in significant additional accumulation of ROS (Fig. 7, Panel B). However, GCN5 inhibition by MB-3 results in a significant increase in oxidative stress, and the combination of SAHA and MB-3 further increases the levels of ROS. Treatment with N-acetylcysteine completely abrogates the growth-inhibitory effect of MB-3 and

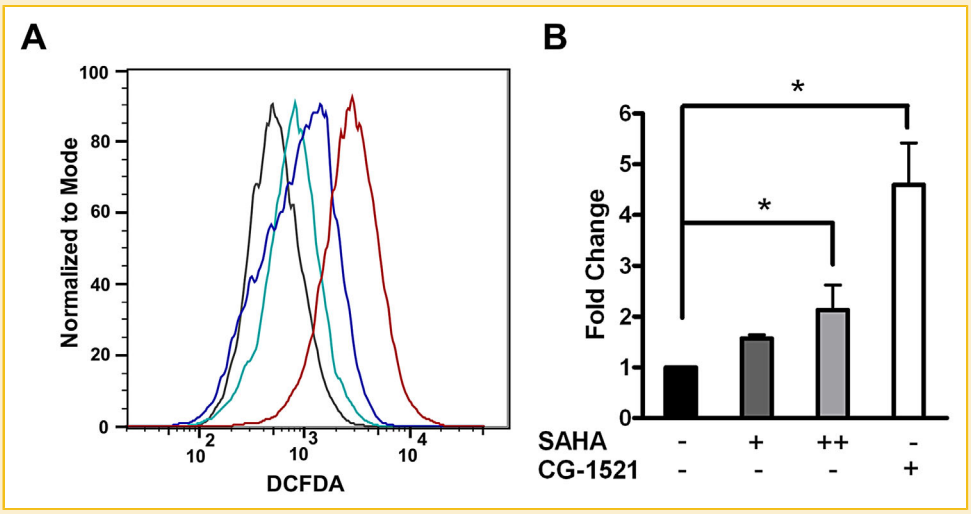

Fig. 6. HDAC inhibitors induce oxidative stress in HT-29 cells. Panel A: HT-29 cells were treated for 24 h with 15 μM CG-1521 (red trace), 2.5 μM SAHA) (light blue trace), 5 μM SAHA (dark blue trace) or vehicle control (black trace). The accumulation of reactive oxygen species was measured after DCFDA staining using flow cytometry as described in Methods. Panel B: The median intensity ratio relative to the control was calculated using the data generated in Panel A.The data are presented as fold change (mean ± SD of 3–5 independent biological replicates and * $P < 0.05$). 15 μM CG-1521 (+), 2.5 μM SAHA (+), 5 μM SAHA (++) or vehicle control (−).

partially alleviates the effect of the combination treatment with HDACi (Fig. 7, Panel C).

DISCUSSION

The data presented here demonstrate that inhibition of GCN5 or PCAF, by siRNA knockdown or chemical inhibition of the enzymatic activity of GCN5, enhances the growth inhibitory activity of CG-1521 and SAHA in yeast, breast and colorectal cancer cells. In yeast, *GCN5* deletion or expression of a catalytic site mutant protein enhances the ability of CG-1521 to induce cell cycle arrest and cell death [Gaupel et al., 2014]. As shown here, this increase in cell death is associated with pronounced ROS generation, including superoxide, in the *gcn5Δ* deletion mutant compared to the wild type. These effects of HDACi are blocked by NAC, indicating that induction of cell death is mediated by oxidative stress. The mechanism of ROS generation appears to be multifactorial. The gene expression profiling described in this manuscript identifies several ontologies related to oxidative stress including oxidation-reduction (GO:0055114) and response to oxidative stress (GO:0006979). Involvement of these ontologies and the induction of thioredoxin- and peroxiredoxin-related genes as well as genes associated with glutamate metabolic processes (GO:0006536), further reinforces the notion that the effects of CG-1521 in yeast are largely mediated by oxidative stress. Notably, deletion mutants of genes upregulated following CG-1521 treatment (*gdh3Δ*, *uga1Δ*, and *uga2Δ*) display increased sensitivity after exposure to oxidative stress [Coleman et al., 2001; Lee et al., 2012] and it has been proposed that Uga2 expression increases after H_2O_2 exposure to elevate NADPH pools [Coleman et al., 2001]. Several studies have also reported a connection between HDAC inhibition and the thioredoxin system. HDAC inhibition by SAHA leads to decreased thioredoxin expression and/or activity and increased thioredoxin-binding protein (TBP-2/TXNIP) expression in transformed cells [Lee et al., 2010a]. In contrast, thioredoxin expression is increased in normal cells, whereas ROS production only occurs in transformed cells [Ungerstedt et al., 2005].

These studies shed light on the well-characterized resistance of normal cells to HDACi relative to transformed cells. In addition to the interaction between HDACi and the thioredoxin system, the class IIb HDACs (HDAC6 and HDAC10) have also been linked to redox regulation. HDAC6 has been shown to down regulate the activity of PrxI and PrxII, members of the peroxiredoxin family that mainly function to reduce hydrogen peroxide (Parmigiani et al., 2008). Knockdown of HDAC10 or treatment with SAHA has also been shown to increase TXNIP expression in gastric cancer cell lines [Butler et al., 2002; Lee et al., 2010b].

In *S. cerevisiae*, genes that are commonly upregulated following environmental stresses are regulated by the SAGA complex [Huisinga and Pugh 2004] and stress related genes, including Tsa2, Ccs1, Gpx2, Grx2, Trx2, and Srx1, are downregulated in a SAGA component mutant background (*tra1Δ*)[Hoke et al., 2008]. In this context deficient transcriptional activation of the oxidative stress response may partially explain differences in oxidative stress levels and cell death after CG-1521 treatment in the wild-type and the *gcn5Δ* deletion mutant. Post-transcriptional events may also contribute to this effect since several studies in yeast have demonstrated that Gcn5 plays an important role in acetylating non-histone proteins, such as the ribosomal protein transcription factor Ifh1 [Downey et al., 2013] and the meiotic transcriptional repressor Ume6 [Mallory et al., 2012].

This study shows that chemical inhibition of GCN5 or knockdown of GCN5 or PCAF expression sensitizes colorectal cancer cells to CG-

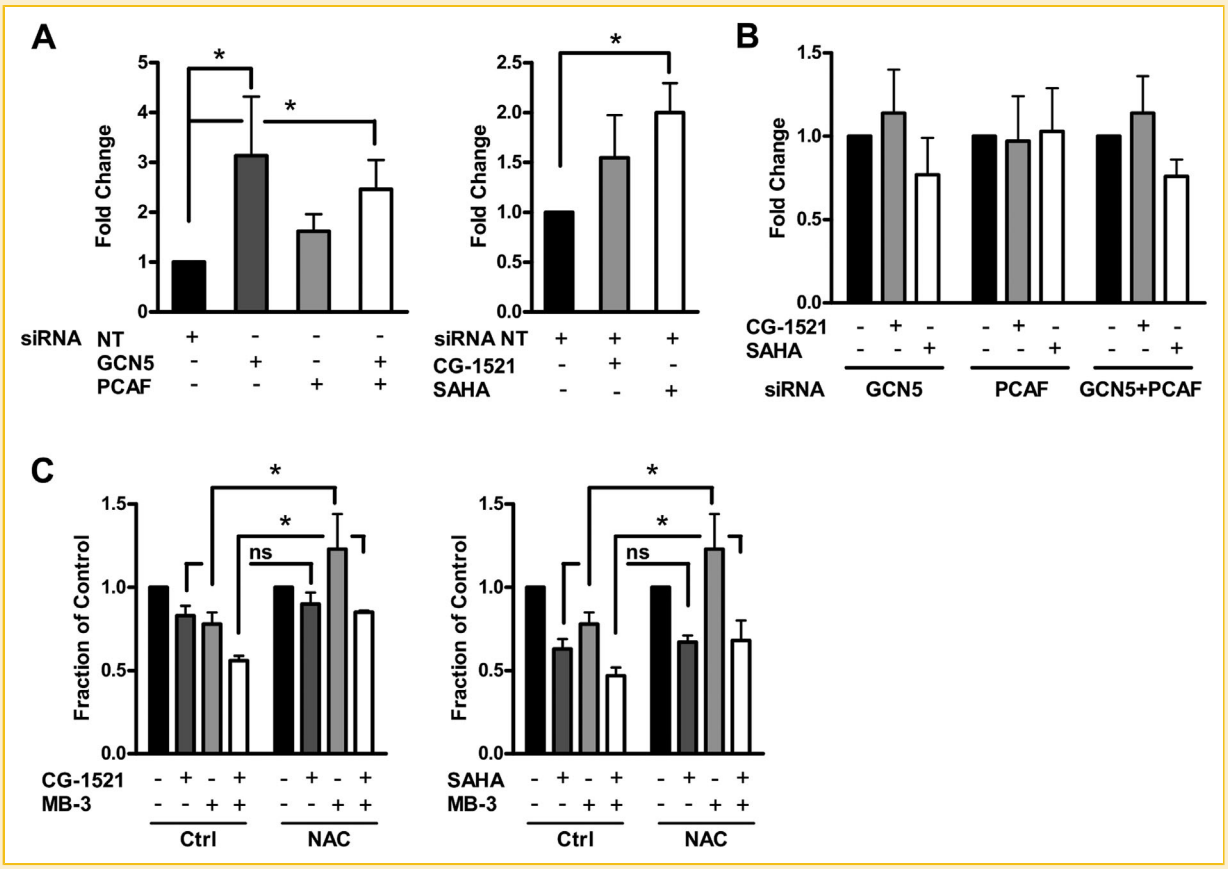

Fig. 7. Inhibition of GCN5 results in an accumulation of ROS intermediates, which is not further exacerbated by HDAC inhibition. Panels A and B: Accumulation of ROS was analyzed after DCFDA staining using flow cytometry. 48 h after siRNA transfection, HT-29 cells were treated with CG-1521 (10μM), SAHA (1.75 μM) or vehicle control for 24 h. Median intensity values were normalized to the non-targeting control (Panel A), or to the vehicle control and non-targeting siRNA control (Panel B) and are presented as fold changes. Panel C: HT-29 cells were treated with 6 μM CG-1521 or 1 μM SAHA and 50 μM MB-3 with or without 7.5 mM N-acetylcysteine (NAC) for 48 h. Nuclei counts were determined using the GE IN Cell Analyzer 2200. The data are normalized to the control and presented as fraction of control (mean ± SD of 3–4 independent biological replicates and * $P < 0.05$).

1521 or SAHA. Loss of either GCN5 or PCAF confers sensitivity to HDAC inhibition, highlighting the fact that these two HATs are not redundant [Xu et al., 2000; Yamauchi et al., 2000; Kikuchi et al., 2005].

In HT-29 colorectal cancer cells SAHA has been shown to induces apoptosis through the generation of ROS, and the associated dissipation of the mitochondrial membrane potential [Portanova et al., 2008]. This study reinforces the correlation of the growth-inhibitory effects with an induction of oxidative stress by both CG-1521 and SAHA in HT-29 cells

HDAC and HAT inhibition appear to cooperate in the activation of cell death pathways in mammalian cells. GCN5 has been reported to be required for cell survival through activation of the PI3K/Akt pathway in response to oxidative stress [Kikuchi et al., 2011b] and PCAF has been shown to inhibit PTEN activity through acetylation, increasing Akt activation and inhibiting G_1 cell cycle arrest [Okumura et al., 2006]. In HT-29 cells, SAHA activates the extrinsic apoptotic pathway through increased expression of the TRAIL receptor DR5 and caspase-8 activation [Portanova et al., 2008]. Taken together, these data suggest that HDAC and HAT inhibition cooperate in the upregulation of several cell death pathways. Notably, in HL-60 cells treatment with TSA coupled with decreased expression of several HATs, including PCAF and GCN5, synergistically increases DR5 levels, promoting apoptosis [Lu et al., 2009].

The human homologues of yeast Gcn5, GCN5 and PCAF, are rarely mutated in cancer suggesting that the downstream effects of CG-1521 mediated through the SAGA complex are unlikely to be disrupted in cancer, and therefore represent an accessible target for many tumor types. These studies highlight the ability of GCN5/PCAF inhibitors and HDAC inhibitors to synergistically reduce cell survival through Akt inhibition and promote cell death through regulation of ROS and death receptor levels, suggesting that simultaneous targeting of HAT and HDAC activities will provide a versatile new approach to cancer therapy.

ACKNOWLEDGMENTS

The authors would like to thank Drs. Randy Morse (Wadsworth Center, New York Department of Health) and Douglas Conklin

(Cancer Research Center, University at Albany) for very useful discussions. The authors would like to thank Jan Baumann for critically reading the manuscript. The authors also acknowledge the outstanding help from Dr. Sridar Chittur, David Frank and Marcy Kuentzel in the Center of Functional Genomics, University at Albany.

REFERENCES

Begley TJ, Rosenbach AS, Ideker T, Samson LD. 2004. Hot spots for modulating toxicity identified by genomic phenotyping and localization mapping. Mol Cell 16:117–125.

Butler LM, Zhou X, Xu W-S, Scher HI, Rifkind RA, Marks PA Richon. 2002. The histone deacetylase inhibitor SAHA arrests cancer cell growth, up-regulates thioredoxin-binding protein-2, and down-regulates thioredoxin. Proc Natl Acad Sci USA 99:11700–11705.

Chatterjee N, Wang WL, Conklin T, Chittur S, Tenniswood M. 2013. Histone deacetylase inhibitors modulate miRNA and mRNA expression, block metaphase, and induce apoptosis in inflammatory breast cancer cells. Cancer Biol Ther 14:658–671.

Cherry JM, Hong EL, Amundsen C, Balakrishnan R, Binkley G, Chan ET, Christie KR, Costazo MC, Dwight SS, Engel SR, Fisk DG, Hirschman JE, Hitz BC, Karra K, Krieger CJ, Miyasato SR, Nash RS, Park J, Skrzypek MS, Simison M, Weng S, Wong ED. 2011. Saccharomyces Genome Database: the genomics resource of budding yeast. Nucleic Acids Res 40:D700–D705.

Coleman ST, Fang TK, Rovinsky SA, Turano FJ, Moye-Rowley WS. 2001. Expression of a glutamate decarboxylase homologue is required for normal oxidative stress tolerance in Saccharomyces cerevisiae. J Biol Chem 276:244–250.

Dekker FJ, Haisma HJ. 2009. Histone acetyl transferases as emerging drug targets. Drug Discov Today 14:942–948.

Downey M, Knight B, Vashisht AA, Seller CA, Wohlschlegel JA, Shore D, Toczyski DP. 2013. Gcn5 and sirtuins regulate acetylation of the ribosomal protein transcription factor Ifh1. Curr Biol 23:1638–1648.

Eberharter AA, Sterner DE, Schieltz D, Hassan A, Yates JR, Berger SL, Workman JL. 1999. The ADA complex is a distinct histone acetyltransferase complex in Saccharomyces cerevisiae. Mol Cell Biol 19:6621–6631.

Eisen MB, Spellman PT, Brown PO, Botstein D. 1998. Cluster analysis and display of genome-wide expression patterns. Proc Natl Acad Sci USA 95:14863–14868.

Garcerá A, Barreto L, Piedrafita L, Tamarit J, Herrero E. 2006. Saccharomyces cerevisiae cells have three Omega class glutathione S-transferases acting as 1 -Cys thiol transferases. Biochem J 398:187–196.

Gaupel AC, Begley T, Tenniswood M. 2014. High throughput screening identifies modulators of histone deacetylase inhibitors. BMC Genomics 15:528.

Grant PA, Duggan L, Côté J, Roberts SM, Brownell JE, Candau R, Ohba R, Owen-Hughes T, Allis CD, Winston F, Berger SL, Workman JL. 1997. Yeast Gcn5 functions in two multisubunit complexes to acetylate nucleosomal histones: Characterization of an Ada complex and the SAGA (Spt/Ada) complex. Genes Dev 11:1640–1650.

Hoke SMT, Guzzo J, Andrews B, Brandl CJ. 2008. Systematic genetic array analysis links the Saccharomyces cerevisiae SAGA/SLIK and NuA4 component Tra1 to multiple cellular processes. BMC Genetics 9:46.

Huisinga KL, Pugh BF. 2004. A genome-wide housekeeping role for TFIID and a highly regulated stress-related role for SAGA in Saccharomyces cerevisiae. Mol Cell 13:573–585.

Kikuchi H, Takami Y, Nakayama T. 2005. GCN5: A supervisor in all-inclusive control of vertebrate cell cycle progression through transcription regulation of various cell cycle-related genes. Gene 347:83–97.

Kikuchi H, Kuribayashi F, Takami Y, Imajoh-Ohmi S, Nakayama T. 2011a. GCN5 regulates the activation of PI3K/Akt survival pathway in B cells exposed to oxidative stress via controlling gene expressions of Syk and Btk. Biochem Biophys Res Commun 405:657–661.

Kikuchi H, Kuribayashi F, Kiwaki N, Takami Y, Nakayama T. 2011b. GCN5 regulates the superoxide-generating system in leukocytes via controlling gp91-phox gene expression. J Immunol 186:3015–3022.

Lee JH, Choy ML, Ngo L, Foster SS, Marks PA. 2010a. Histone deacetylase inhibitor induces DNA damage, which normal but not transformed cells can repair. Proc Natl Acad Sci USA 107:14639–14644.

Lee JH, Jeong EG, Choi MC, Kim SH, Park JH, Song SH, Park J, Bang YJ, Kim TY. 2010b. Inhibition of histone deacetylase 10 induces thioredoxin-interacting protein and causes accumulation of reactive oxygen species in SNU-620 human gastric cancer cells. Mol Cells 30:107–112.

Lee YJ, Kim KJ, Kang HY, Kim H-R, Maeng PJ. 2012. Involvement of GDH3-encoded NADP+- dependent glutamate dehydrogenase in yeast cell resistance to stress-induced apoptosis in stationary phase cells. J Biol Chem 287:44221–44233.

Livak KJ, Schmittgen TD. 2001. Analysis of relative gene expression data using real-time quantitative PCR and the 2(-Delta Delta C(T)) Method. Methods 25:402–408.

Lu MC, Du YC, Chuu JJ, Hwang SL, Hsieh PC, Hung CS, Chang FR, Wu YC. 2009. Active extracts of wild fruiting bodies of Antrodia camphorata (EEAC) induce leukemia HL 60 cells apoptosis partially through histone hypoacetylation and synergistically promote anticancer effect of trichostatin A. Arch Toxicol 83:121–129.

Mallory MJ, Law MJ, Sterner DE, Berger SL, Strich R. 2012. Gcn5p-dependent acetylation induces degradation of the meiotic transcriptional repressor Ume6p. Mol Biol Cell 23:1609–1617.

Mann BS, Johnson JR, Cohen MH, Justice R, Pazdur R. 2007. FDA approval summary: vorinostat for treatment of advanced primary cutaneous T-cell lymphoma. Oncologist 12:1247–1252.

Okumura K, Mendoza M, Bachoo RM, DePinho RA, Cavenee WK, Furnari FB. 2006. PCAF modulates PTEN activity. J Biol Chem 281:26562–26568.

Outten CE, Falk RL, Culotta VC. 2005. Cellular factors required for protection from hyperoxia toxicity in Saccharomyces cerevisiae. Biochem J 388:93–101.

Parmigiani RB, Xu WS, Venta-Perez G, Erdjument- Bromage H, Yaneva M, Tempst P, Marks PA. 2008. HDAC6 is a specific deacetylase of peroxiredoxins and is involved in redox regulation. Proc Natl Acad Sci U S A 105:9633–9638.

Portanova P, Russo T, Pellerito O, Calvaruso G, Giuliano M, Vento R, Tesoriere G. 2008. The role of oxidative stress in apoptosis induced by the histone deacetylase inhibitor suberoylanilide hydroxamic acid in human colon adenocarcinoma HT-29 cells. Int J Oncol 33:325–331.

Qiu T, Zhou L, Zhu W, Wang T, Wang J, Shu Y, Liu P. 2013. Effects of treatment with histone deacetylase inhibitors in solid tumors: A review based on 30 clinical trials. Future Oncol 9:255–269.

Rozen S, Skaletsky H. 2000. Primer3 on the WWW for general users and for biologist programmers. Methods Mol Biol 132:365–386.

Slingerland M, Guchelaar HJ, Gelderblom H. 2014. Histone deacetylase inhibitors: an overview of the clinical studies in solid tumors. Anticancer Drugs 25:140–149.

Ungerstedt JS, Sowa Y, Xu W-S, Shao Y, Dokmanovic M, Perez G, Ngo L, Holmgren A, Jiang X, Marks PA. 2005. Role of thioredoxin in the response of normal and transformed cells to histone deacetylase inhibitors. Proc Natl Acad Sci USA 102:673–678.

VanderMolen KM, McCulloch W, Pearce CJ, Oberlies NH. 2011. Romidepsin (Istodax, NSC 630176, FR901228, FK228, depsipeptide): A natural product recently approved for cutaneous T-cell lymphoma. J Antibiotics 64: 525–531.

West AC, Johnstone RW. 2014. New and emerging HDAC inhibitors for cancer treatment. J Clin Invest 124:30–39.

Xu W, Edmondson DG, Evrard YA, Wakamiya M, Behringer RR, Roth SY. 2000. Loss of Gcn5l2 leads to increased apoptosis and mesodermal defects during mouse development. Nature Genet 26:229–232.

Yamauchi T, Yamauchi J, Kuwata T, Tamura T, Yamashita T, Bae N, Westphal H, Ozato K, Nakatani Y. 2000. Distinct but overlapping roles of histone acetylase PCAF and of the closely related PCAF- B/GCN5 in mouse embryogenesis. Proc Natl Acad Sci USA 97:11303–11306.

SUPPORTING INFORMATION

Additional supporting information may be found in the online version of this article at the publisher's web-site